Deformation due to contact between a rough surface and a smooth ball

J. Jamari *, D.J. Schipper

*Surface Technology and Tribology Section, Faculty of Engineering Technology, University of Twente,
Drienerloolaan 5, Postbus 217, 7500 AE, Enschede, The Netherlands*

Abstract

Theoretical and experimental results are presented to evaluate the deformation behavior of the contact between a real rough flat surface and a smooth ball. There are three deformation responses: plastic deformation of the asperities only, plastic deformation of the bulk only and combined plastic deformation of both the asperities and the bulk. The effects of the surface roughness and the Hertzian contact parameters on the effective contact pressure are presented. The experimental results confirmed the theoretical prediction very well. For a given Hertzian contact situation the surface roughness plays an important role in controlling the deformation behavior of the contacting surfaces. A criterion is presented to predict the deformation behavior of contacting engineering surfaces.
© 2006 Elsevier B.V. All rights reserved.

Keywords: Contact mechanics; Indentation; Plastic deformation; Asperity

1. Introduction

When two engineering surfaces are pressed together there will always be some contact deformation. Depending on the contact condition, these contact deformation can be categorized as macro-contact or micro-contact. The contact between a heavily loaded roller and the inner and outer race ways in a rolling-element bearing, for example, can be analyzed as a macroscopic contact when omitting the effect of surface roughness. In the Hertz theory, the contact of two elastic bodies is based on the assumption that their surfaces are topographically smooth [1]. However, most engineering surfaces are rough on micro-scale. High points or micro-protrusions, usually called asperities, exist on all engineering solid surfaces irrespective of their method of production. In non-lubricated or boundary lubrication systems, when such surfaces are loaded against each other, the actual contact takes place at these asperities, i.e. micro-contacts.

During the contact of two surfaces, contact will initially occur at a limited amount of asperities of different shapes and sizes to support the normal load [2–4]. The number of asperities in contact becomes larger as the normal load is increased. Deformation occurs in the region of contact spots, establishing stresses

that oppose the applied load. If the deformation is in the same order as the topography of the surfaces, the response to the normal load may be strongly related to the height and size of the asperities. For an elastic–plastic deforming material the plasticity may be initiated either at the surface (asperities) or in the bulk depending on the contact condition. This problem is of particular interest to tribologists and engineers with respect to the functional properties of devices. Or in another words, depending on the desired functional performance specific contacting surfaces may be designed.

The analytical and numerical modeling for estimating the actual pressure distribution for the contact of various surface profiles have been studied by many researchers [5–14]. Greenwood and Williamson [5] studied the contact between two nominally flat surfaces. They assumed that the flat surface is covered with hemi-spherical asperities and the heights of the asperities are represented by a well-defined statistical distribution function (i.e. Gaussian). As an extension, by using the same approach, Greenwood and Tripp (GT model) [6] analyzed the contact problem of a smooth spherical surface against a plane covered with asperities and Lo [7] analyzed the contact of two parallel rough cylinders. Mikic and Roca [8] studied the contact problem of two rough spherical surfaces based on the plasticity theory.

Most of the developed contact models are devoted to the calculation of the real contact area, load carrying capacity or sub-surface stresses. The deformation behavior of the contacting

---

* Corresponding author. Tel.: +31 53 4892463; fax: +31 53 4894784.
E-mail address: j.jamari@ctw.utwente.nl (J. Jamari).

Nomenclature

A_0	unit area
d	cut-off height
E	reduced elastic modulus
$E_{1,2}$	elastic moduli surface 1 and 2
H	hardness
K	hardness coefficient
$\mathbf{K}(k)$	first kind complete elliptical integral
N	number of asperities
p	effective pressure
p_0	maximum Hertzian contact pressure
$p(0)$	effective central pressure
P	contact load
r	radial coordinate
R	radius of the sphere indenter
w_b	surface or bulk deformation
y	profile coordinate in loading direction
z	asperity height

Greek letters

α	non-dimensional roughness parameter
β	average asperity radius
$\phi(z)$	statistical distribution of asperity height
η_s	asperity density, N/A_0
μ	non-dimensional asperity density parameter
$\nu_{1,2}$	Poisson's ratio
ω_a	asperity deformation

surfaces is rarely explored, especially during unloading. Rajendrakumar and Biswas [9] have studied the deformation response of the contact between a two-dimensional rough surface and a smooth cylinder. A map which can be used as a design guide for predicting the deformation responses (asperity or bulk deformation) of the contacting surfaces was constructed. However, the map was based upon a simple two-dimensional configuration of the contact problem and there is no experimental verification. The asperities are represented by uniformly spaced cylinders of the same radius and height.

This paper offers a new criterion for surface deformation for the contact of three-dimensional real rough surfaces. A sphere and a flat rough surface contact configuration was chosen because it is found commonly in many engineering applications such as the contact of a ball on the race way of ball bearings, ball screws, ball joint, etc.

2. Theoretical background

In the case of the contact between a sphere and a flat rough surface, true contact is not made continuously over the circular contact area envisaged by the Hertz theory but through an archipelago of small discrete islands roughly clustered within a circular region. Therefore, true contact pressure is discontinuous, very high within the contact region and falling to zero in between the contact islands. In the present analysis of the con-

tact between a rough surface and a smooth ball, the GT model is used for convenience.

By using iterative numerical techniques Greenwood and Tripp [6], see Appendix A, solved Eqs. (A.5)–(A.7) to find the effective pressure distribution $p(r)$. The solution depends upon two independent non-dimensional parameters α and μ:

$$\alpha = \sigma_s \left(\frac{16RE^2}{9P^2} \right)^{1/3} \tag{1}$$

$$\mu = \frac{8}{3} \eta_s \sigma_s (2R\beta)^{1/2} \tag{2}$$

where σ_s is the r.m.s. roughness of the summits, R the radius of the sphere, E the reduced elasticity modulus, P the normal load, η_s the number of asperity per unit area and β is the radius of the asperities.

Fig. 1 shows the calculation results of GT [6] expressed by the ratio of the central effective pressure $p(0)$ and the maximum Hertzian pressure p_0 as a function of the parameter α for two values of μ which bracket most practical engineering surfaces. It is clear from Fig. 1 that the parameter α is the primarily governing factor to predict the effect of surface roughness on the effective contact pressure while the detailed geometry of the surface expressed by the parameter μ has a secondary effect. The effective pressure decreases as the roughness increases, and consequently, the ratio of the deformation of the asperities to the bulk increases. This contact problem has also been analyzed by Mikic and Roca [8] by assuming that the asperity deforms plastically. Interestingly, results showed that the difference between their theory and the GT theory is very small.

Plastic deformation is particular of interest for engineers since it changes the mechanical component permanently. Therefore, plastic deformation of the bulk of the contacting surfaces will be discussed further in the present analysis. In general, for smooth surfaces the initial yielding occurs when the maximum
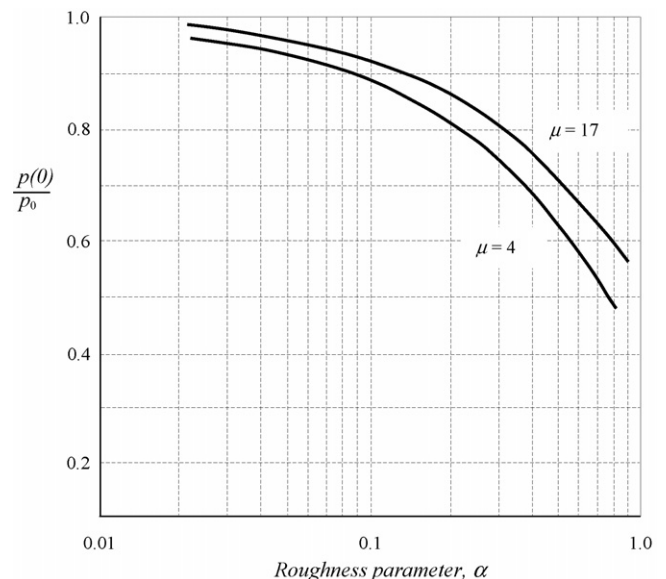

Fig. 1. Ratio of central effective pressure to maximum Hertz pressure as a function of roughness parameter α and μ, after [3,6].

or central Hertz pressure:

$$p_{0-y} = KH \tag{3}$$

Tabor [10] proposed that the value K in Eq. (3) is to be 0.6. Another researchers found that the K value depend on the Poisson's ratio ν. Chang et al. [11], for instance, found by using the von Mises failure criteria that $K = 0.454 + 0.41\nu$ while Lin and Lin [12] defined $K = 0.4645 + 0.3141\nu + 0.1943\nu^2$. However, the difference of the K value between those three models is small.

In this paper, a combination of the relation of Tabor [10] and the graph of GT [6] is proposed by which one is able to predict for given contact conditions the contact deformation behavior. In other words, if the effective maximum or central pressure is larger than KH bulk plastic deformation occurs and if the effective central pressure is lower than KH plastic deformation may happen at asperity level. The experimental results to verify the proposed combination of the GT and Tabor model will be presented in the next section.

3. Experimental work

3.1. Specimens

Hardened steel spheres ($H = 7.5$ GPa, $E = 210$ GPa and $\nu = 0.3$) with a diameter of 10 mm were used as a hard smooth spherical indenter. The deformable flat specimens used were made from aluminium ($H = 0.24$ GPa, $E = 75.2$ GPa and $\nu = 0.34$) and brass ($H = 1.2$ GPa, $E = 105$ GPa and $\nu = 0.34$). The sphere specimens have a center line average roughness R_a of about 0.01 μm and the average roughness of the flat specimens varied from about 0.1 to 2.3 μm.

3.2. Matching and stitching

In most practical situations it is not possible to get an accurate or detailed image of a complete cross-section of the contact area. To determine an accurate image of the cross-section a high lateral resolution is needed and as a result only small areas can be measured due to the limitation of the hardware. To overcome this problem Sloetjes et al. [13,14] developed a new measuring technique by matching and stitching a number of small but detailed images together from sequence measurements.

The matching of two images can be defined as aligning or repositioning the overlapping part of two successive images. The stitching process itself in fact is the matching process of several images in order to get a detailed and wide image of a complete section across the contact area. Several measurements are taken in the stitching process and each one having a certain overlap area with the previous one. For every stitching of the subsequence two images the mutual translation and rotation can be determined based on the overlapping area (matching process). Once all the images are matched, one large image is created as a complete of the stitching process. Fig. 2 shows schematically the matching and stitching procedure used in the present experiments. As can be seen in this schematically representation, the predicted contact area (shown by the dashed line) from the static
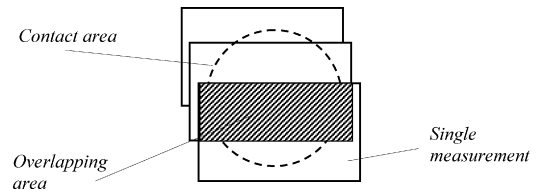

Fig. 2. Matching and stitching procedure, schematically.

compression of the sphere is wider than one single measurement of the optical profiler therefore the matching and stitching procedure is applied. This process is carried out for before and after an experiment. To get the difference image between before and after loading/indentation the two large images are matched.

3.3. Experimental details

Experiments were performed on a setup as shown in Fig. 3. The maximum load which could be applied to this setup was about 300 N. Before doing any test, the spherical and flat specimens were cleaned with acetone and dried in air. A new flat surface is used for every single indentation test.

An optical interference microscope was used to measure the three-dimensional surface roughness. An X–Y table which is controlled by stepper motors was employed to positioning the flat specimen from the loading position (position A) to the surface measuring position (position A') and the other way around. The measurement sequence is as follows. First, the flat surface was measured under the optical interference microscope. The number of the stitching images which should be taken depends on the predicted contact area and the chosen magnification of the interferometer. After finishing the surface measurement in position A' the flat surface was moved to the loading position A. In this loading position the statically mounted sphere specimen was moved down by the loading screw and subsequently loaded by the dead weight load system. To reduce the effect of friction the contact region was lubricated. The load
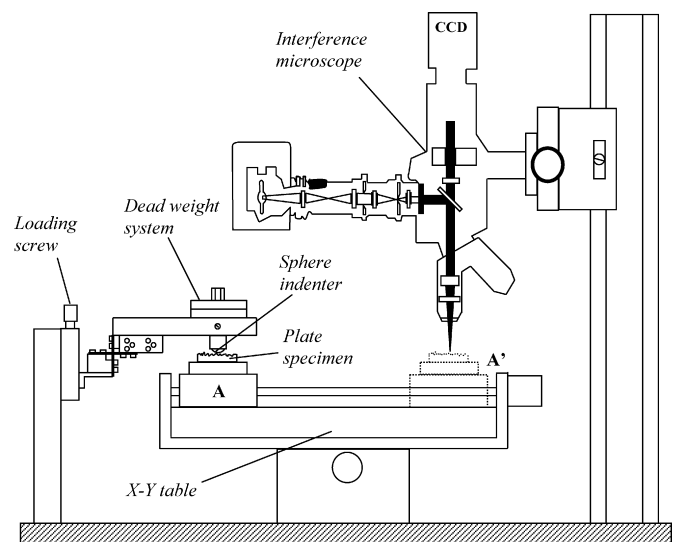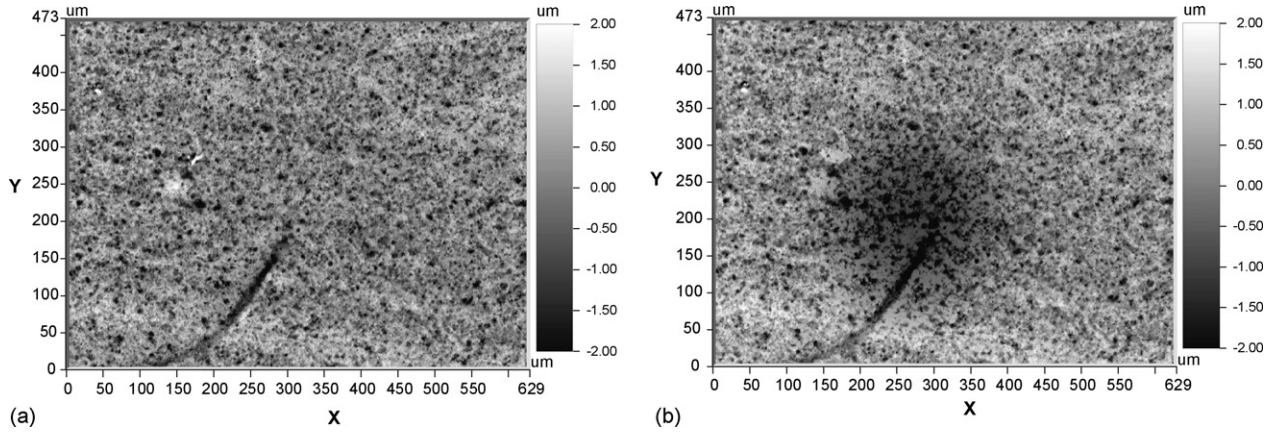

Fig. 3. Experimental setup.

Fig. 4. Surface measurements of an aluminium flat surface $R_q = 0.67\,\mu$m, load $= 4$ N, $\alpha = 0.86$ and $\mu = 6$. (a) Before indentation experiment and (b) after indentation experiment.

was applied to the sphere specimen for 30 s and then unloaded. Prior to measuring the after loading contact area with the optical interference microscope, again the sphere was cleaned and dried. After taking all the surface images data the matching and stitching calculation was performed separately by a personal computer.

4. Experimental results

4.1. Experiment on aluminium surfaces

Fig. 4 shows the measurements results of the aluminium flat surfaces before and after an experiment for load $= 4$ N, $\alpha = 0.86$ and $\mu = 6$. The matching and stitching results of this surface can be seen in Fig. 5a. It is clear from Fig. 5 that bulk deformation occurs as indicated by the different datum of the difference image following the shape of the spherical indenter. Fig. 5b shows this phenomenon more clearly. As can be seen, the asperities are almost undeformed whereas it is clear that the bulk is deformed. This is referred to as asperity persistence where the plastic deformation of the asperity is very small compared to the bulk deformation.

Fig. 6 shows the example of the matching and stitching of the experimental results where deformation takes place both in the asperities and bulk. In this case, the asperities and bulk deformation are comparable, therefore, in the difference image (Fig. 6a) the shape of the bulk deformation like in Fig. 5a is present along with the local shape like archipelago which corresponds to the difference of the asperity deformation.

An example of experimental results of plastic deformation on asperity level without any bulk plastic deformation of the aluminium surface is shown in Fig. 7. Here, the bulk deformation is not present as can be seen in the difference image of Fig. 7a. The deformation occurs in the asperities only.

For all the experimental results, it can be seen that the matching and stitching performance is very good. The presence of a small scatter in the difference profile is due to the noise of the measurement. However, the important information or the global shape of the difference profile is very clear so that the plastic deformation behavior can be evaluated easily.

It should be noted here that for all the present experiments the value of σ_s was taken from the r.m.s. roughness of the surface [15]. The parameters η_s and β were calculated based on "nine point summit" method [16] in order to determine the parameter μ.

4.2. Experiment on brass surfaces

Similar results were also found for the brass surfaces. The surface measurement results of the brass for load $= 12$ N, $\alpha = 0.09$
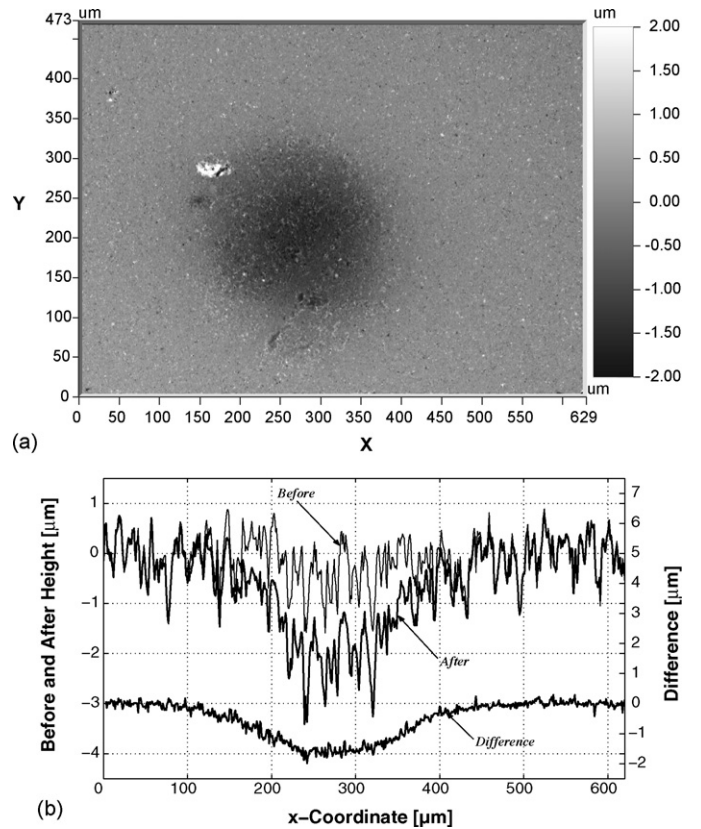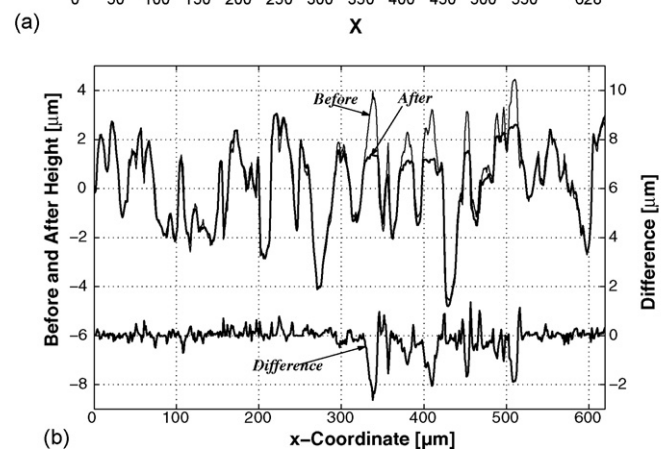

Fig. 5. Matching and stitching results of an aluminium surface $R_q = 0.67\,\mu$m, load $= 4$ N, $\alpha = 0.86$ and $\mu = 6$. (a) Difference 3D image of Fig. 4 and (b) profile at $y = 200\,\mu$m.

(a)

(b)
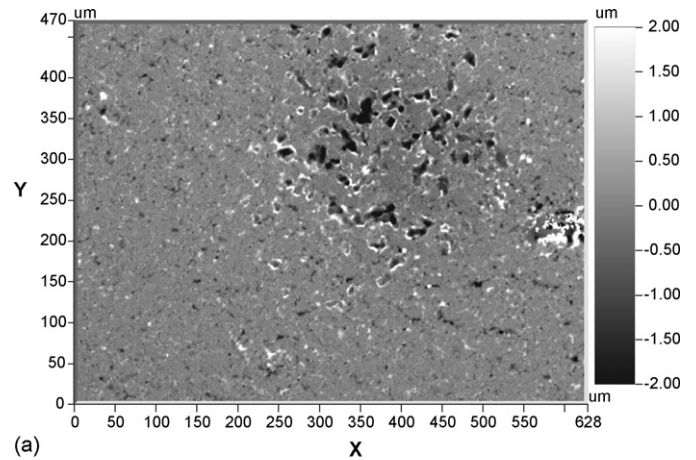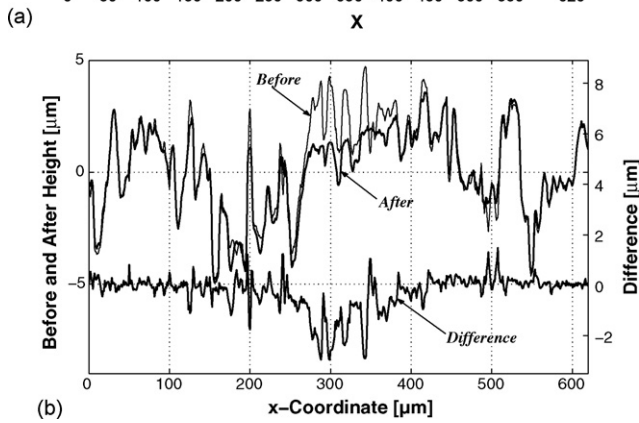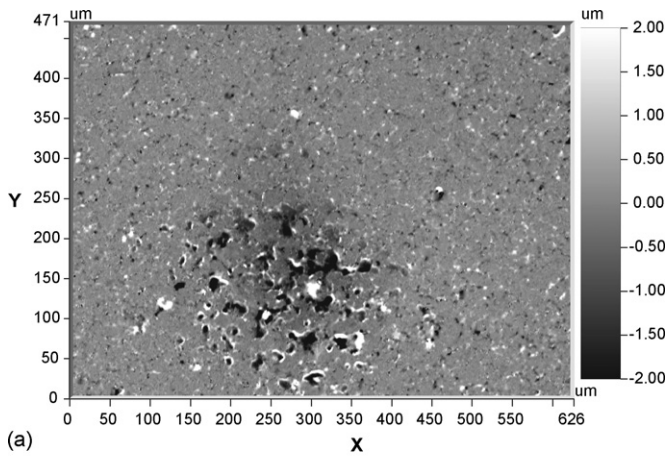
Fig. 6. Matching and stitching results of an aluminium surface $R_q = 2.1\,\mu m$, load = 4 N, $\alpha = 2.7$ and $\mu = 10$. (a) Difference 3D image and (b) profile at $y = 158\,\mu m$.

(a)

(b)

Fig. 7. Matching and stitching results of an aluminium surface $R_q = 2.2\,\mu m$, load = 4 N, $\alpha = 2.84$ and $\mu = 12$. (a) Difference 3D image and (b) profile at $y = 320\,\mu m$.

and $\mu = 11$ are shown in Fig. 8. Example results of the matching and stitching results for bulk deformation, combined bulk and asperity deformation and asperity deformation are shown in Figs. 9–11, respectively.

5. Discussion

Experimental results showed that even for the same Hertzian contact pressure the plastic deformation state behaves differently depending on the roughness of the surfaces. The parameter α increases proportionally to the roughness of the surfaces, and as a result, the central effective pressure decreases. According to Eq. (3) plasticity of the bulk surface may take place when this central effective pressure is larger than the constant K times the hardness of the flat surface H. The experimental results presented are in line with the theoretical prediction of α in Eq. (1) and the central effective pressure curves of Fig. 1. It is unimportant
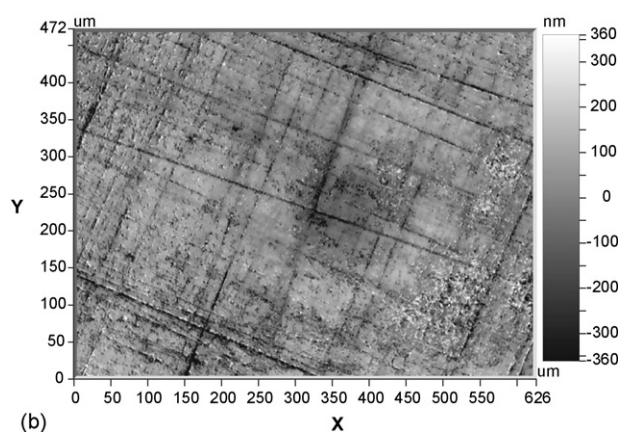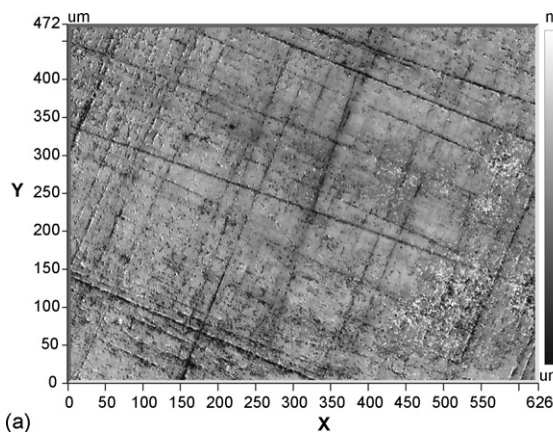

(a)

(b)

Fig. 8. Surface measurements of a brass flat surface $R_q = 0.13\,\mu m$, load = 12 N, $\alpha = 0.09$ and $\mu = 11$. (a) Before indentation experiment and (b) after indentation experiment.

(a)

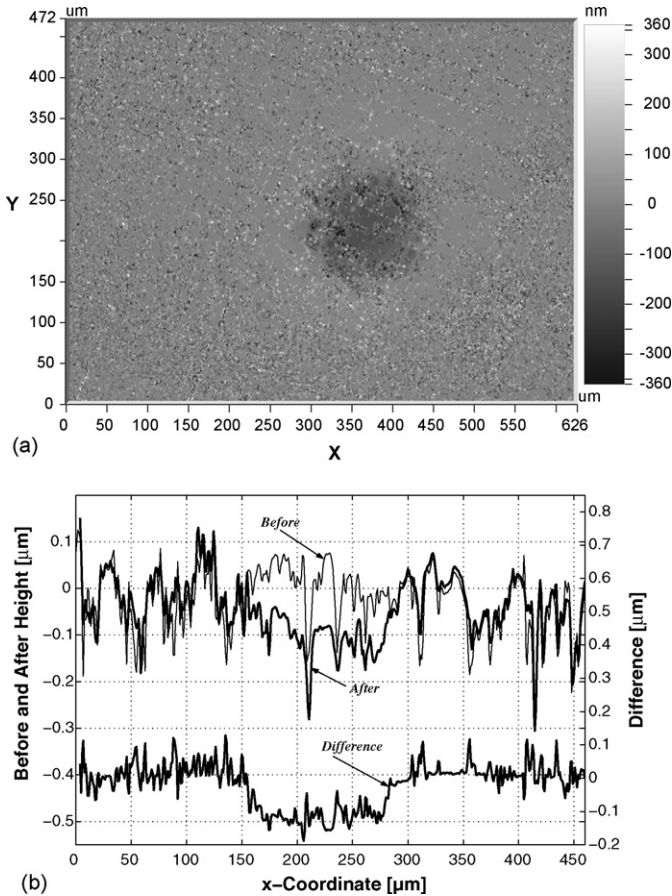
(b)

Fig. 9. Matching and stitching results of a brass surface $R_q = 0.13 \, \mu m$, load = 12 N, $\alpha = 0.09$ and $\mu = 11$. (a) Difference 3D image of Fig. 8 and (b) profile at $x = 380 \, \mu m$.

whether the asperities deform elastically [6] or plastically [8] in this statistical approach.

The results also showed the minor effect of the parameter μ. For bulk deformation of brass as was shown in Fig. 9, for instance, the parameter $\mu = 11$ which corresponds to the fraction of the central effective pressure and the maximum Hertz pressure $p(0)/p_0$ of about 0.925 ($\alpha = 0.09$). If the parameter μ is taken to be 4 the ratio $p(0)/p_0 = 0.9$ and when the parameter μ is equal to 17 the ratio $p(0)/p_0 = 0.93$ for the same α. Indeed, the difference
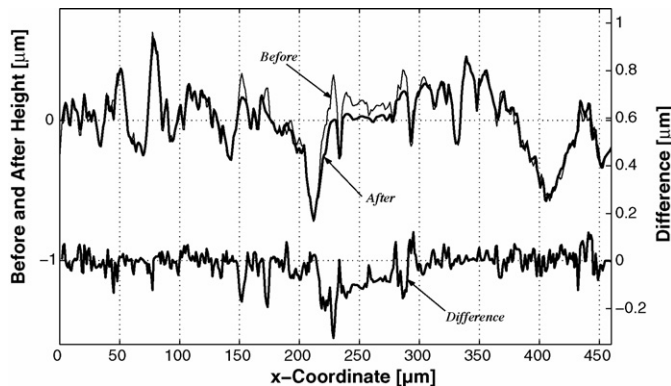

Fig. 10. Profile of the matching and stitching results of a brass surface $R_q = 0.28 \, \mu m$, load = 12 N, $\alpha = 0.2$ and $\mu = 13$.
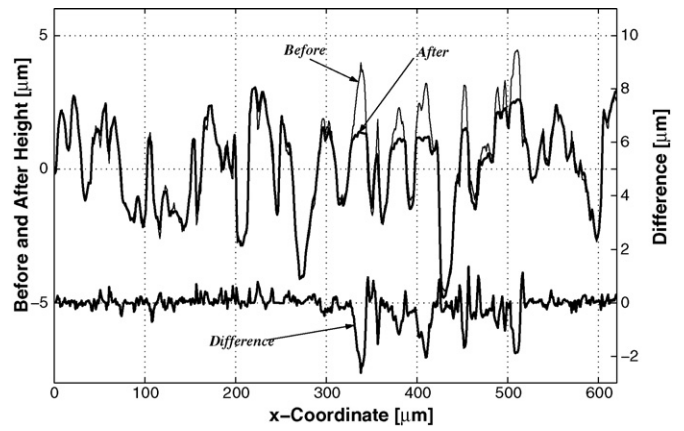

Fig. 11. Profile of the matching and stitching results of a brass surface $R_q = 0.7 \, \mu m$, load = 12 N, $\alpha = 0.5$ and $\mu = 7$.

in the ratio $p(0)/p_0$ becomes larger when the two extremes of the parameter μ are taken as the parameter α increases, however, the difference is not that dramatically.

Many experiments were performed in order to gain more insightful results for a certain range of surface roughness. These results are presented in Fig. 12 where $p(0)/H$ is plotted as a function of the surface roughness R_q. In this figure the points Al_A, Al_B, Al_{AB}, Br_A, Br_{AB} and Br_B correspond the contact condition locations of aluminium and brass as was shown in Figs. 5–7 and 9–11 (the index A, B and AB refer to asperity, bulk and combined asperity–bulk plastic deformation, respectively). The figure shows that for contact conditions located above the ratio $p(0)/H = 0.6$ bulk plastic deformation is observed while below the ratio $p(0)/H = 0.6$ asperity deformation is attained for the whole range of the surface roughness tested. For the contact conditions near the line $p(0)/H = 0.6$ comprises the deformation behavior of the asperity and the bulk.
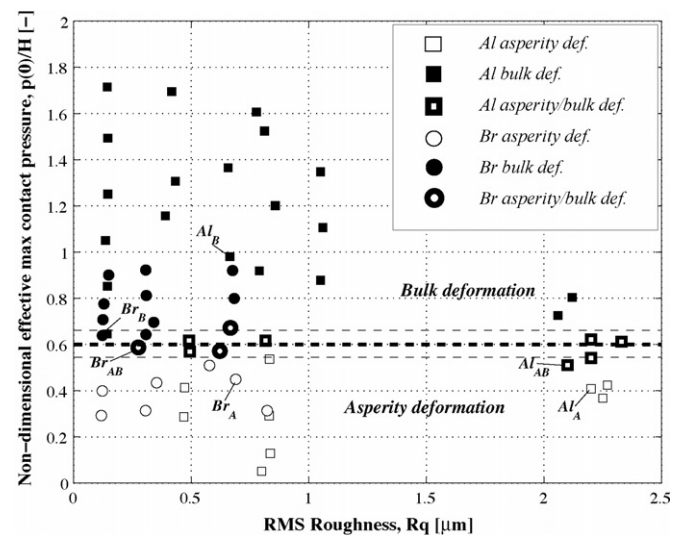

Fig. 12. Plastic deformation behavior of the contact between a rough surface and a smooth curved body. Square symbols are for aluminium and circle symbols are for brass where the full filled symbols indicating bulk deformation, the open symbols indicate asperity deformation and the half-filled symbols represent a combined deformation of the asperity and the bulk.

It can be concluded from above discussion that the central effective pressure of the contact between two rough surfaces can be correlated to the contact of two smooth bodies by introducing the parameters α and μ. For practical engineering purposes it is very convenience to build an expression in determining the value of the ratio $p(0)/p_0$ instead of using the graph in Fig. 1. Since the parameter μ has a secondary effect to the ratio $p(0)/p_0$ and for $\mu = 4$ and 17 brackets most of the engineering surfaces a curve was found to fit the GT data as:

$$\frac{p(0)}{p_0} = 1 - \exp\left(-\frac{2}{3\alpha^{3/5}}\right) \tag{4}$$

Using Eq. (4) and the plasticity condition of Eq. (3), a criterion can be made for asperity deformation to occur as:

$$\frac{p_0}{H}\left[1 - \exp\left(-\frac{2}{3\alpha^{3/5}}\right)\right] < K \tag{5}$$

where $K = 0.6$ and p_0 is the maximum Hertz pressure:

$$p_0 = \left(\frac{16PE^2}{\pi^3 R^2}\right) \tag{6}$$

6. Conclusion

An experimental investigation was carried out to study the deformation behavior of the contact between a real rough surface and a smooth ball. The experimental results confirmed the proposed criterion very well.

The main finding of the present work is that the surface roughness is the primarily factor in controlling the deformation behavior of contacting surfaces. For a given Hertzian contact pressure situation the deformation behavior differs significantly.

For the purpose of engineering application, a formula is developed, Eq. (5), to predict the deformation behavior of contacting engineering surfaces.

If the ratio $p(0)/H$ is larger than 0.6 bulk deformation occurs and if the ratio $p(0)/H$ is lower than 0.6 asperity deformation takes place. Combination between of asperity and the bulk deformation occurs at the ratio $p(0)/H \approx 0.6$.

Acknowledgements

Appendix A

According to the GT model [6] the asperities are assumed to have spherical caps of uniform radius β, whose heights above a mean datum have a statistical distribution $\phi(z)$ deform elastically and independently following the Hertz theory. The contact load P required to compress an individual asperity by an amount of ω_a is given by:

$$P_a = \frac{4}{3}E\beta^{1/2}\omega_a^{3/2} \tag{A.1}$$

E is the effective elastic modulus defined as:

$$\frac{1}{E} = \frac{1 - v_1^2}{E_1} + \frac{1 - v_2^2}{E_2} \tag{A.2}$$

where E_1 and E_2, and v_1 and v_2 are Young's moduli and Poisson's ratios of the two materials in contact, respectively. If such a nominally flat rough surface is in contact with a smooth flat surface at a separation d, the effective pressure p between them is:

$$p = \frac{4}{3}\eta_s E\beta^{1/2}\int_d^\infty (z - d)^{3/2}\phi(z)\,dz \tag{A.3}$$

where η_s is the asperity density, i.e. the number of asperity per unit area N/A_0.

The geometry of the contact of a rough surface with a smooth sphere is shown diagrammatically in Fig. A.1. A datum is taken at the mean level of the rough surface. For the sphere, the profile of the undeformed sphere relative to the datum is defined by:

$$y = y_0 - \frac{r^2}{2R} \tag{A.4}$$

When the contacting surfaces start to be compressed there will be deformations in the asperities ω_a and a deformation of the bulk w_b, hence the separation between the two surfaces is given by:

$$d(r) = w_b(r) - y(r) = -y_0 + \frac{r^2}{2R} + w_b(r) \tag{A.5}$$

If the asperity deformation is assumed to be elastic, substituting of Eq. (A.5) into Eq. (A.3) yields the effective pressure at radius r as:

$$p(r) = \frac{4}{3}\eta_s E\beta^{1/2}\int_d^\infty \{z_s - d(r)\}^{3/2}\phi(z_s)\,dz_s \tag{A.6}$$

where z_s is the height of the asperity summit above the datum. The bulk deformation w_b is related to the effective pressure $p(r)$ by the equations for the axi-symmetric deformation of an elastic
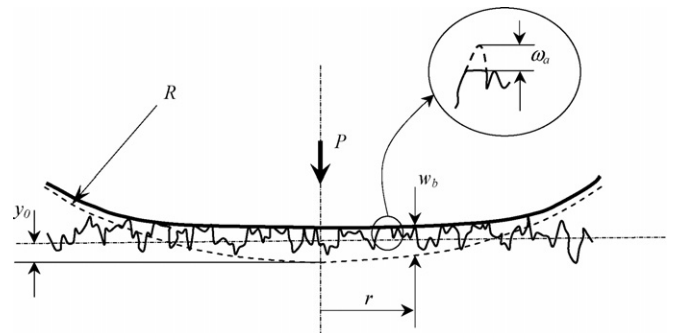

Fig. A.1. Contact of a nominally flat rough surface with a smooth sphere, after [3,6].

half-space [3] and is written as:

$$w_{\mathrm{b}}(r) = \frac{4}{\pi E} \int_0^a \frac{t}{t+r} p(t) \mathbf{K}(k) \, \mathrm{d}t \tag{A.7}$$

where $\mathbf{K}$ is the first kind complete elliptical integral with argument k:

$$k = \frac{2(rt)^{1/2}}{r+t} \tag{A.8}$$

References

[1] S. Timoshenko, J.N. Goodier, Theory of Elasticity, McGraw-Hill Book Company Inc., New York, 1951.

[2] T.R. Thomas, Rough Surfaces, Longman, London, 1982.

[3] K.L. Johnson, Contact Mechanics, Cambridge University Press, Cambridge, UK, 1985.

[4] D.J. Whitehouse, Handbook of Surface Metrology, Institute of Physics Publishing, Bristol, UK, 1994.

[5] J.A. Greenwood, J.B.P. Williamson, Contact of nominally flat surfaces, Proc. R. Soc. Lond. Ser. A295 (1966) 300–319.

[6] J.A. Greenwood, J.H. Tripp, The elastic contact of rough spheres, Trans. ASME, J. Appl. Mech. 34 (1967) 153–159.

[7] C.C. Lo, Elastic contact of rough cylinders, Int. J. Mech. Sci. 11 (1969) 105–115.

[8] B.B. Mikic, R.T. Roca, A solution to the contact of two rough spherical surfaces, Trans. ASME, J. Appl. Mech. 96 (1974) 801–803.

[9] P.K. Rajendrakumar, S.K. Biswas, Deformation due to contact between a two-dimensional rough surface and a smooth cylinder, Tribol. Lett. 3 (1997) 297–301.

[10] D. Tabor, The Hardness of Metals, Oxford University Press, 1951.

[11] W.R. Chang, I. Etsion, D.B. Bogy, Static friction coefficient model for metallic rough surfaces, Trans. ASME, J. Tribol. 110 (1988) 57–63.

[12] L.P. Lin, J.F. Lin, An elastoplastic microasperity contact model for metallic materials, Trans. ASME, J. Tribol. 127 (2005) 343–354.

[13] J.W. Sloetjes, D.J. Schipper, P.M. Lugt, J.H. Tripp, The determination of changes in surface topography using image processing techniques, in: Proceeding of the International Tribology Conference, Nagasaki, 2000.

[14] J.W. Sloetjes, Y.C. Tasan, M.B. de Rooij, D.J. Schipper, Algorithm for determining changes in micro-geometry using image processing techniques, in: Proceeding of the 2nd Asia International Conference on Tribology, Cheju Island, Korea, Asiatrib'02, 2002.

[15] J.A. Greenwood, K.L. Johnson, E. Matsubara, A surface roughness parameter in hertz contact, Wear 100 (1984) 47–57.

[16] J.A. Greenwood, A unified theory of surface roughness, Proc. R. Soc. Lond. Ser. A393 (1984) 133–157.